

# Optimization of Linear Parameterizable $\mathcal{H}_\infty$ Controllers in the Frequency Domain

E. van Solingen\* J.W. van Wingerden\* R. De Breuker\*  
M. Verhaegen\*

\* Delft University of Technology, Delft, 2628 CD, The Netherlands  
(e-mail: E.vanSolingen@tudelft.nl).

---

**Abstract:** In this paper a novel approach for  $\mathcal{H}_\infty$  controller design for linear parameterizable controllers is presented. The approach uses the generalized Nyquist stability criterion to find the parameters of linear parameterized controllers for Multi-Input Multi-Output (MIMO) systems. The main advantage of the proposed approach is that the generalized plant does not have to be diagonally dominant and that there is no need for a desired open-loop response function. By constraining the Nyquist curve from certain parts in the frequency domain, controller parameters that guarantee stability and performance of the closed-loop system can be found. The method is successfully applied to two cases involving a double-mass-spring-damper system. In the first case only controller parameters are optimized and in the second case both structural and controller parameters are optimized.

---

## 1. INTRODUCTION

In recent years several developments have been made in fixed-structure robust control synthesis. The main reason for these developments is that classical optimal and robust control design techniques lead to high order controllers (e.g., see Zhou et al. [1996]). Due to the high order of the controller, which makes tuning very difficult, this type of controllers is typically not implemented in industrial applications. Furthermore, often, the structure of the controller is already known beforehand (e.g., PID controllers). For that reason, low-order and fixed-structure robust control techniques were designed and developed in e.g., Hol [2006]. The main problem that arises when constraining the structure and order of the controller is that the optimization problem is no longer convex and sometimes considered as NP-hard, see Nemirovskii [1993].

Several approaches for fixed-structure robust controller design exist. In Safonov et al. [1994], bilinear matrix inequality techniques are used for robust controller synthesis and in Apkarian and Noll [2006] nonsmooth cost functions are minimized for  $\mathcal{H}_\infty$  controller synthesis. The latter method can both be used with frequency domain representations as well as with state-space domain parameterizations of the unknown controller. Another approach is presented by Galdos et al. [2010], Karimi and Galdos [2010], where robust controllers are designed using the (generalized) Nyquist stability criterion. The approach taken in the latter references is to represent the  $\mathcal{H}_\infty$  robust performance condition as a set of linear or convex constraints with respect to the controller parameters. Furthermore, in Hast et al. [2013] a convex-concave optimization procedure for PID controller design is outlined, evolutionary algorithms

are used in Popov and Werner [2006] and randomized algorithms are used in Maruta et al. [2009] to find fixed-structure robust controllers that satisfy  $\mathcal{H}_\infty$ -norm specifications.

In this paper, a novel approach for  $\mathcal{H}_\infty$  controller design is presented, which follows a paradigm similar to Galdos et al. [2010], Karimi and Galdos [2010]. The main idea is to find the parameters of linearly parameterized controllers such that the Nyquist diagram of the determinant of a certain MIMO frequency response function does not encircle the origin. By using the generalized Nyquist stability criterion and by using robust control theory (e.g., Skogestad and Postlethwaite [2006]), conditions can be formulated for both stability and performance. The controller is parameterized such that a diagonal structure is obtained with only the controller parameters on the diagonal. To prevent the Nyquist plot from encircling the critical point, (multilinear) constraints are formulated in the frequency domain.

The outlined approach also allows for structural parameter optimization. That is, by extracting structural parameters from the plant, the diagonal controller structure can be extended with these parameters. Extracting the parameters can be done by using LFT techniques (see e.g., [Redheffer, 1960, Zhou and Doyle, 1998]). The approach to optimize the controller parameters extended with the structural parameters remains unchanged, such that both structural and controller parameters can be simultaneously optimized. The property to design controlled systems more efficiently in an integrated manner (see e.g., Camino et al. [2003]) is very appealing.

The approach presented in this paper differs from Galdos et al. [2010], Karimi and Galdos [2010] in the sense that it does not require a diagonally dominant plant or a decoupling procedure of the plant in the controller design

---

\* This work is funded and supported by the Far and Large Offshore Wind (FLOW) program, *Integrated design of far large offshore wind turbines*

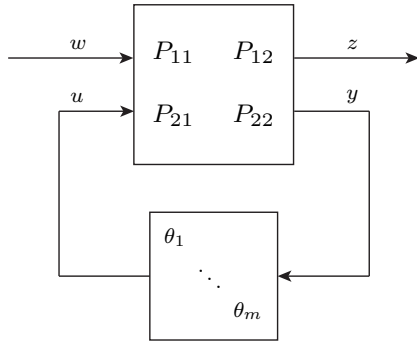


Fig. 1. Generalized plant with linear parameterized controller.

process. Moreover, in Galdos et al. [2010], Karimi and Galdos [2010] a desired open-loop transfer function is required in order to find the  $\mathcal{H}_\infty$  controller, whereas in our approach this is not required.

The paper is divided into several sections. In Section 2, the problem is formulated and conditions for stability and performance are formulated. Then, in Section 3, the constraints are formulated and the optimization problem is outlined. The method is demonstrated in Section 4 on a double-mass-spring-damper system in which two cases are considered. In the first case, the objective is to find the controller parameters that satisfy a performance specification and in the second case both structural and controller parameters are sought that satisfy the performance specification. Finally, the paper is concluded in Section 5.

## 2. PROBLEM FORMULATION

In this section the approach to develop an efficient frequency domain based controller synthesis method is formulated. The formulation is started by defining the generalized plant and linear controller parameterization, after which conditions for nominal stability and performance are stipulated.

We consider the following partitioning of the generalized plant

$$\begin{bmatrix} z \\ y \end{bmatrix} = \underbrace{\begin{bmatrix} P_{11}(s) & P_{12}(s) \\ P_{21}(s) & P_{22}(s) \end{bmatrix}}_{P(s)} \begin{bmatrix} w \\ u \end{bmatrix}, \quad (1)$$

with  $z \in \mathbb{R}^{n_z}$ ,  $w \in \mathbb{R}^{n_w}$ ,  $y \in \mathbb{R}^{n_m}$ , and  $u \in \mathbb{R}^{n_m}$ . The transfer functions  $P_{11}(s)$ ,  $P_{12}(s)$ ,  $P_{21}(s)$  and  $P_{22}(s)$  have corresponding dimensions and are all assumed to be stable. The controller parameters are real scalars, i.e.,  $\theta_i \in \mathbb{R}$ . With these definitions the controller is defined as

$$u = \underbrace{\begin{bmatrix} \theta_1 & 0 \\ \vdots & \vdots \\ 0 & \theta_m \end{bmatrix}}_K y. \quad (2)$$

The plant and controller structure as defined in (1) and (2) for a PID controller can be obtained as follows. Let a PID controller be given by

$$K_{\text{PID}}(s) = K_p + \frac{K_i}{s} + \frac{K_d s}{T_f s + 1}. \quad (3)$$

Then, a diagonal structure with the controller parameters as in Fig. 2 is obtained in a straightforward manner,

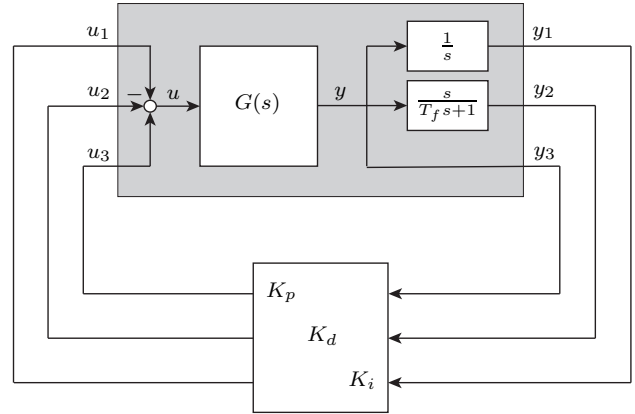


Fig. 2. Linear parameterization of a PID controller.

assuming  $T_f$  is given. Notice that such a structure can also be obtained from, among others, notch filters, low-pass and high-pass filters and lead-lag compensators (see e.g., van Solingen and van Wingerden [2014]).

The goal is now to find an  $\mathcal{H}_\infty$  controller that achieves performance, i.e., when  $\|T_{wz}\|_\infty < 1$ , where  $T_{wz}$  is given by

$$T_{wz}(s) = F_l(P, K) = P_{11} + P_{12}K(I - P_{22}K)^{-1}P_{21}.$$

For a freely-parameterized controller  $K$ , this problem is convex (Zhou et al. [1996]), but leads to a solution having the same order as the generalized plant, which is typically not desired in practical applications. On the other hand, for a fixed-structure controller, the problem is no longer convex, and advanced and sophisticated optimization routines are required to find the optimal controller (see e.g., Hol [2006], Apkarian and Noll [2006]).

In order to find an  $\mathcal{H}_\infty$  controller, consider the following approach, assuming a stable<sup>1</sup> generalized plant  $P(s)$  and given the frequency response data of  $P(s)$  denoted by  $P(j\omega)$ . By making use of the generalized Nyquist stability criterion of MacFarlane and Postlethwaite [1977] we formulate two conditions.

**Stability** The closed-loop system in Fig. 1 is asymptotically stable if for a given stable generalized plant  $P(j\omega)$ , the Nyquist plot of

$$\det \left( I - \begin{bmatrix} \theta_1 & & 0 \\ & \ddots & \\ 0 & & \theta_m \end{bmatrix} P_{22}(j\omega) \right), \quad \forall \omega, \quad (4)$$

does not encircle the origin;

**Performance** The closed-loop system in Fig. 3 has performance if  $\|T_{wz}\|_\infty < 1$ . This is achieved if for a given stable generalized plant  $P(j\omega)$ , the Nyquist plot of

$$\det \left( I - \begin{bmatrix} \frac{\Delta_P(j\omega)}{0} & 0 \\ 0 & \begin{bmatrix} \theta_1 & 0 \\ \vdots & \vdots \\ 0 & \theta_m \end{bmatrix} \end{bmatrix} P(j\omega) \right), \quad \forall \omega, \Delta_P(j\omega), \quad (5)$$

does not encircle the origin for  $\Delta_P \in \mathbb{C}^{n_w \times n_z}$  and  $\|\Delta_P(s)\|_\infty \leq 1$ .

<sup>1</sup> In this paper only stable generalized plants are considered, however the method can be extended to include unstable generalized plants.

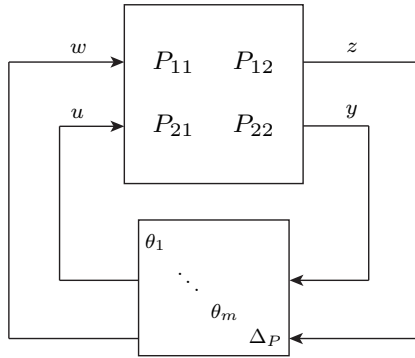


Fig. 3. Configuration for performance

Note that the system in Fig. 3 is obtained by including in Fig. 1 a perturbation block  $\Delta_P(j\omega)$  in feedback with the exogenous input  $w$  and exogenous output  $z$ . The performance condition (5) can be deduced from robust control theory (e.g., refer to Skogestad and Postlethwaite [2006]) and is omitted for brevity.

Now the task at hand is to find the controller parameters  $\theta$  such that the Nyquist curve satisfies the condition in (4) for stability and the condition in (5) for performance.

### 3. FEASIBILITY PROBLEM

In the previous section, the conditions for closed-loop stability and performance are given. In this section the stability (4) and performance condition (5) are formulated into a feasibility problem. It is shown how the constraints of the feasibility problem are related to the controller parameters.

#### 3.1 Determinant expression

From the determinant conditions in (4) and (5) it can be shown that the determinant expression has a structure which is *multilinear* in the controller parameters. That is, consider the case of ( $m = 2$ ) controller parameters and the following partitioning of  $P_{22}(s)$

$$P_{22}(j\omega) = \begin{bmatrix} P_{22}^{(11)}(j\omega) & P_{22}^{(12)}(j\omega) \\ P_{22}^{(21)}(j\omega) & P_{22}^{(22)}(j\omega) \end{bmatrix},$$

where  $P_{22}^{(\cdot)} \in \mathbb{C}$ . Then, the determinant expression of (4) can be written as

$$Q(\theta, j\omega) = 1 - P_{22}^{(11)}(j\omega)\theta_1 - P_{22}^{(22)}(j\omega)\theta_2 + \left( P_{22}^{(11)}(j\omega)P_{22}^{(22)}(j\omega) - P_{22}^{(12)}(j\omega)P_{22}^{(21)}(j\omega) \right) \theta_1\theta_2 \quad (6)$$

From the above expression it can be seen that there are no self-multiplications and is in fact bilinear in the controller parameters  $\theta$ . Due to the determinant, a multilinear expression is obtained for higher number of controller parameters.

The previous case can be extended to also include performance. In condition (5) it is stated, that for all  $\|\Delta_P(s)\|_\infty \leq 1$ , the Nyquist plot should not encircle the origin. Hence, for the performance condition of (5), an expression  $Q_\Delta(\theta, j\omega)$  similar to (6) can be obtained by evaluating (5). The expression then obtained also involves terms with  $P_{11}(j\omega)$ ,  $P_{12}(j\omega)$ ,  $P_{21}(j\omega)$  and  $\Delta_P(j\omega)$ .

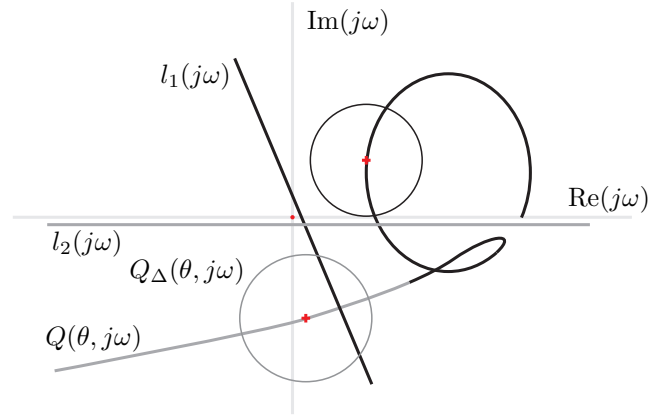


Fig. 4. Nyquist diagram for  $Q(\theta, j\omega)$  (stability) and  $Q_\Delta(\theta, j\omega)$  (performance). The colors indicate which of the constraints  $l_1(j\omega)$  and  $l_2(j\omega)$  hold for which part of the Nyquist plots.

Likewise, the expression for  $Q_\Delta(\theta, j\omega)$  is multilinear in the controller parameters  $\theta$ .

#### 3.2 Constraints

To prevent the Nyquist plot from encircling the origin, the determinant expressions  $Q(\theta, j\omega)$  and  $Q_\Delta(\theta, j\omega)$  are constrained from some parts in the Nyquist diagram. This is schematically shown in Fig. 4, in which the Nyquist curves  $Q(\theta, j\omega)$  and  $Q_\Delta(\theta, j\omega)$  of a loop transfer function is shown. In the figure the loop transfers are such that the Nyquist plot does not encircle the origin. Hence, both the stability condition (4) and performance condition (5) are satisfied. To obtain a loop transfer function of which the Nyquist curve does not encircle the origin, the constraints  $l_1(j\omega)$  and  $l_2(j\omega)$  are introduced (see Fig. 4). The constraint  $l_1(j\omega) < Q_\Delta(\theta, j\omega)$  is such that  $Q_\Delta(\theta, j\omega)$  for higher frequencies is constrained from the origin. The constraint  $l_2(j\omega) > Q_\Delta(\theta, j\omega)$  is introduced such that encirclement of the origin is also avoided for lower frequencies. In the remainder of this paper we will use  $Q_\Delta(\theta, j\omega)$  to refer to the determinant of the loop transfer function including the performance  $\Delta_P(j\omega)$ .

The previously mentioned constraints are lines in the Nyquist diagram with a certain slope  $\alpha$  and offset  $c$ , i.e.,

$$\text{Im}(j\omega) = \alpha \text{Re}(j\omega) + c, \quad (7)$$

where  $\text{Re}(\cdot)$  and  $\text{Im}(\cdot)$  denote the real and imaginary parts, respectively. Then, if one wants to have the Nyquist curve  $Q_\Delta(\theta, j\omega)$  below this line, this can be achieved by plugging the real and imaginary parts of the determinant  $Q_\Delta(\theta, j\omega)$  into (7) to obtain

$$l(\theta, j\omega) = \text{Im}(Q_\Delta(\theta, j\omega)) - \alpha \text{Re}(Q_\Delta(\theta, j\omega)) - c < 0. \quad (8)$$

A similar expression is found if one wants to constrain the determinant above a line.

#### 3.3 Feasibility problem

The determinant denoted by  $Q_\Delta(\theta, j\omega)$  is, among others, determined by the performance  $\Delta_P(j\omega)$ , which is described by the infinite set of complex numbers satisfying  $\|\Delta_P(s)\|_\infty \leq 1$ . To avoid having an infinite number of constraints, the performance  $\Delta_P(j\omega)$  is realized by  $n_d$

points randomly drawn from the infinite set. Now, denote a realization of the performance  $\Delta_P(j\omega)$  by  $\bar{\Delta}_P(j\omega)$  and the determinant determined by  $\bar{\Delta}_P(j\omega)$  by  $Q_{\bar{\Delta}}(\theta, j\omega)$ . Then, performance for  $Q_{\bar{\Delta}}(\theta, j\omega)$ , subject to the constraint in (8), can be written as a large feasibility test.

**Feasibility problem**

$$\text{Find } \theta \text{ such that } l(\theta, j\omega) < 0 \quad \forall \omega, \bar{\Delta}_P(j\omega). \quad (9)$$

Notice that the feasibility problem (9) can be constructed as in Fig. 4, such that a line constraint can be assigned per frequency  $\omega$ .

4. RESULTS

In this section, the approach outlined in Section 2 and Section 3 is applied to find a controller for a double-mass-spring damper system. Two cases are considered, i.e.,

- (1) Find the controller parameters for an upper bound on the sensitivity function;
- (2) Find the controller parameters and a structural parameter for an upper bound on the sensitivity function.

The two cases are outlined in Section 4.1 and Section 4.2.

4.1 Case 1: Double-mass-spring-damper system

The double-mass-spring-damper system can be modelled by means of two masses  $m_1$  and  $m_2$  connected through a spring  $k$  and a damper  $d$ , as illustrated in Fig. 5. The system has the applied force  $F$  as input and the measured position  $x_2$  as output. A PD controller acts on the position  $x_2$  of the second mass  $m_2$ . The transfer function from the force input  $F$  to the measured position  $x_2$  of mass  $m_2$  is given by

$$G(s) = \frac{x_2}{F} = \frac{ds + k}{m_1 m_2 s^4 + (m_1 + m_2) ds^3 + (m_1 + m_2) k s^2}.$$

A first-order Padé approximation is used to include a time delay of  $T_d = 0.1$  s. The output of the system  $y = x_2$  is connected to a PD controller given by

$$PD(s) = K_p \frac{1}{0.01s + 1} + K_d \frac{s}{0.01s + 1}. \quad (10)$$

In order to maintain a diagonal control structure with only the controller parameters on the diagonal, the fractions in (10) are absorbed into the plant. Then, a bound is put on the sensitivity function by means of a second-order performance weight as in Skogestad and Postlethwaite [2006]

$$W_p(s) = \frac{s^2 / M_p^2 + 2\beta_p \omega_B + \omega_B^2}{s^2 + 2\beta_p A_p \omega_B + (A_p \omega_B)^2},$$

where  $\beta_p = 0.3$ ,  $M_p = 2$ ,  $A_p = 1 \cdot 10^{-3}$  and  $\omega_B = 0.1$ . The complete interconnection structure of the system with the PD controller and performance weight is shown in Fig. 6, where also the perturbation  $\Delta_P$  is included. In this example the parameter values were taken as  $m_1 = m_2 = k = 1$  and  $d = 0.05$ .

Since the complexity of this problem is relatively low (only two controller parameters need to be found), a grid search of the controller parameters is carried out. For a number of combinations of  $K_p$  and  $K_d$ , the stability of the closed-loop system is evaluated and the  $\mathcal{H}_\infty$ -norm is computed.

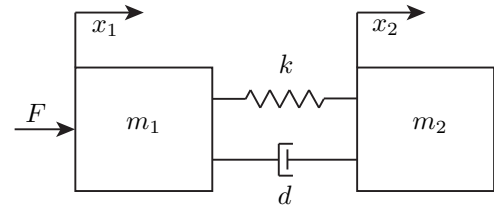


Fig. 5. Example case 1: double-mass-spring-damper

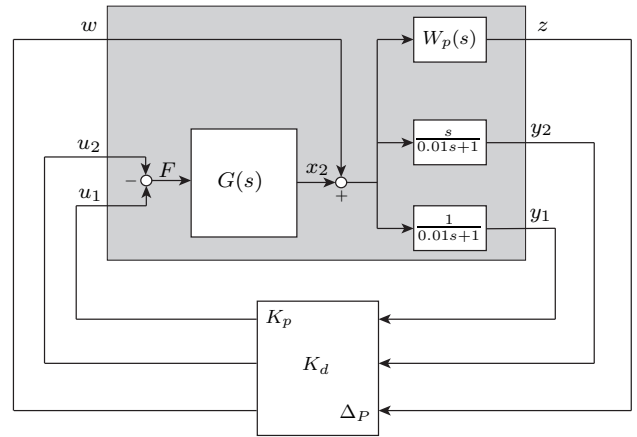


Fig. 6. Configuration of the plant and controller for the double-mass-spring damper system.

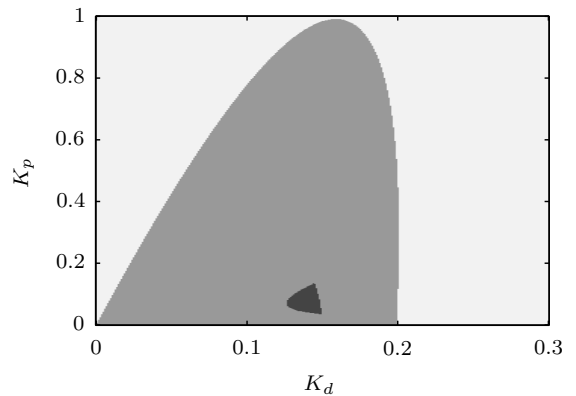


Fig. 7. Results of the grid search of  $K_p$  and  $K_d$  for the controlled double-mass-spring-damper system. The light grey area represents controller parameter combinations resulting in an unstable closed-loop system, the grey area are combinations which yield a stable closed-loop system and the dark grey area are the solutions with  $\mathcal{H}_\infty$ -norm lower than 1.

The results of this analysis are shown in Fig. 7. It can be observed that there is not an obvious solution to obtain an  $\mathcal{H}_\infty$ -norm lower than 1, making it an interesting problem to evaluate the proposed controller design method.

The feasibility problem in (9) is then turned into an optimization problem as follows. Since the generalized plant is stable, the Nyquist curve should not encircle the origin. From some trial-and-error combinations of  $K_p$  and  $K_d$  a general idea of the Nyquist curve was obtained (similar to Fig. 4). With this knowledge, two constraints in the Nyquist diagram are formulated, i.e.,

Table 1. Optimization results

Description	$\mathcal{H}_\infty^{\min}$	$\mathcal{H}_\infty^{\max}$	Success [%]
Nyquist optim. ( $n_d = 10$ )	0.935	9.280	72
Nyquist optim. ( $n_d = 25$ )	0.934	1.021	96
Nyquist optim. ( $n_d = 50$ )	0.935	0.968	100
Nyquist optim. ( $n_d = 100$ )	0.940	0.952	100
Nyquist optim. ( $n_d = 250$ )	0.940	0.942	100

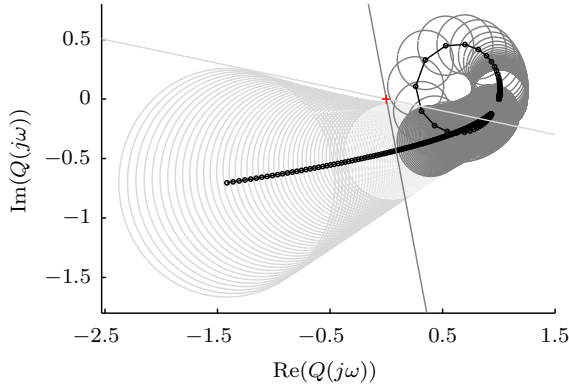


Fig. 8. Resulting Nyquist plots of  $Q(\theta, j\omega)$  (black) and  $Q_\Delta(\theta, j\omega)$  (light grey and dark grey) for the double-mass-spring-damper system. The line colors of the constraints are matched with  $Q_\Delta(\theta, j\omega)$  to indicate where they hold.

$$\begin{aligned} \text{Im}(Q_\Delta(j\omega)) + 0.2\text{Re}(Q_\Delta(j\omega)) - 0.001 < 0 & \text{ for } \omega \leq 0.16, \\ -\text{Im}(Q_\Delta(j\omega)) - 5\text{Re}(Q_\Delta(j\omega)) + 0.001 < 0 & \text{ for } \omega \geq 0.20. \end{aligned}$$

The performance  $\Delta_P(j\omega)$  is for each  $\omega$  realized by  $n_d$  points randomly sampled on the unit circle using a uniform distribution. We consider  $N = 400$  complex frequencies on a logarithmic scale in the interval  $[0.1, 10]$  rad/s. The optimization problem is solved with the MATLAB `fmincon` function (for which an interior-point optimization algorithm was selected). The optimization procedure is carried out for 100 Monte Carlo simulations<sup>2</sup> with random initial controller parameters and the parameters are bounded by  $K_p \in [0, 1]$  and  $K_d \in [0, 0.3]$ . The objective function<sup>3</sup> of the optimization procedure is chosen as

$$\min K_p^2 + K_d^2. \quad (11)$$

The results obtained using `fmincon` are listed in Table 1, from which it can be seen that for increasing  $n_d$  the success rate increases (i.e., better realized  $\Delta_P(j\omega)$  yield  $\|T_{wz}(j\omega)\|_\infty \leq 1$ ). The Nyquist diagram of the plant with controller (for  $n_d = 250$ ) giving the minimum cost (for which  $\|T_{wz}\|_\infty = 0.9296$ ,  $K_p = 0.0479$  and  $K_d = 0.1454$ ) is shown in Fig. 8, where it can be seen that the performance circles do not encircle the origin (indicated by +).

<sup>2</sup> In each Monte Carlo simulation the  $n_d$  performance  $\bar{\Delta}_P$ 's are redrawn on the unit circle.

<sup>3</sup> Remark that the objective function is not necessary. We could equally well have opted for a feasibility problem of finding  $K_p$  and  $K_d$  that satisfies the performance condition. Further remark that the objective function can be chosen differently.

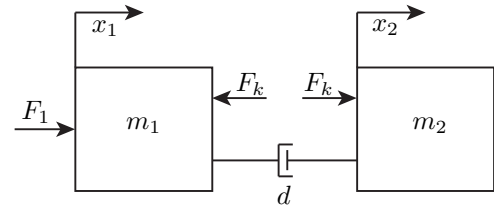


Fig. 9. Example case 2: double-mass-damper with additional external force input  $F_k$ .

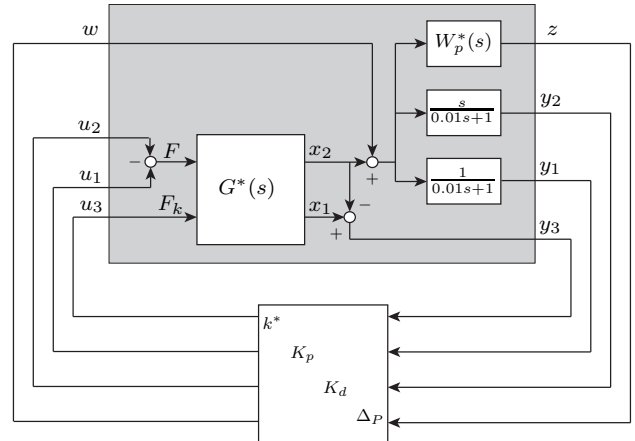


Fig. 10. Configuration of the plant and controller for the double-mass-damper system.

#### 4.2 Case 2: Double-mass-damper system

In the second case a double-mass-damper system is considered. The spring  $k$  is removed from the system in Fig. 5 and an external force  $F_k$  is subjected to both masses (see Fig. 9). The dynamics for the modified system  $G^*(s)$  are given by

$$\begin{bmatrix} x_1 \\ x_2 \end{bmatrix} = \frac{ds + k}{m_1 m_2 s^3 + (m_1 + m_2) ds^2} \begin{bmatrix} m_2 s + d & -m_2 s \\ d & m_1 s \end{bmatrix} \begin{bmatrix} F \\ F_k \end{bmatrix}$$

Note that by taking

$$F_k = k^*(x_1 - x_2), \quad (12)$$

and setting  $k^* = k$ , the systems in Fig. 5 and Fig. 9 are identical. If  $F_k$  is chosen as in (12), it can be regarded as adding stiffness to the system. Thus, by absorbing  $x_1 - x_2$  into the plant,  $k^*$  becomes an additional parameter which can be optimized.

As with the previous case, a PD controller is used. In order to avoid trivial solutions (i.e., from  $k^*$  going to infinity), the performance weight  $W_p(s)$  of the previous case is modified to

$$W_p^*(s) = W_p(s) \times \frac{s^2 + 2\beta_p^* A_p^* \omega_B^* + (A_p^* \omega_B^*)^2}{s^2 / (M_p^*)^2 + 2\beta_p^* \omega_B^* + (\omega_B^*)^2},$$

where  $\beta_p^* = 0.7$ ,  $M_p^* = 1.9$ ,  $A_p^* = 0.9$  and  $\omega_B^* = 1$ . The modification can be regarded as putting a constraint on the resonance frequency of the system. With the modified performance weight  $W_p^*$ , the generalized plant is then depicted in Fig. 10. Similar to the previous case, a grid search of the three controller parameters is carried out in order to visualize the solution space. The results are shown in Fig. 11.

Now the proposed method is applied to this case to find the controller parameters  $K_p$ ,  $K_d$  and  $k^*$  that satisfy the

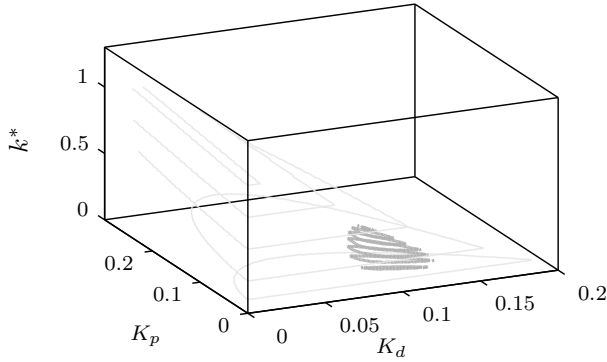


Fig. 11. Results of the grid search of  $K_p$ ,  $K_d$  and  $k^*$  for the double-mass-damper system. The volume within the light grey contour lines indicate the parameter combinations resulting in a stable closed-loop system and the volume within the dark grey contour lines are combinations which yield a stable closed-loop system with  $\mathcal{H}_\infty$ -norm lower than 1.

performance condition (5). The performance  $\Delta_P(j\omega)$  is realized by  $n_d = 50$  points randomly sampled on the unit circle and the following constraints are applied

$$\begin{aligned} -\text{Im}(Q_\Delta(j\omega)) + 0.7\text{Re}(Q_\Delta(j\omega)) + 0.001 < 0 & \text{ for } \omega \leq 0.39, \\ \text{Im}(Q_\Delta(j\omega)) + 0.001 < 0 & \text{ for } 0.51 \leq \omega \leq 0.54. \end{aligned}$$

Then, 100 Monte Carlo simulations for random initial points were performed, the parameters are bounded by  $K_p \in [0, 1]$ ,  $K_d \in [0, 0.3]$ ,  $k^* \in [0, 2.5]$ , and the objective function<sup>4</sup> is chosen as

$$\min K_p^2 + K_d^2 + (k^*)^2.$$

The solution with the lowest objective function has controller parameters  $K_p = 0.0461$ ,  $K_d = 0.1031$ ,  $k^* = 0.1145$ , and  $\|T_{wz}\|_\infty = 0.9217$ . Due to space constraints the resulting Nyquist curve is not shown.

## 5. CONCLUSIONS

A new method to design linear parameterizable robust controllers is proposed. The method exploits the generalized Nyquist stability criterion. Both stability and performance conditions are formulated, which can be fulfilled by introducing constraints in the Nyquist diagram. Using the constraints a multilinear feasibility problem can be formulated, after which the controller parameters satisfying the conditions can be found. The method allows the controller parameters to be extended with structural parameters such that an integrated design procedure of plant and controller is possible. The method is successfully demonstrated on two examples where in the first controller parameters are optimized and in the second both structural and controller parameters are optimized.

<sup>4</sup> Again the objective function can be chosen differently.

## REFERENCES

- P. Apkarian and D. Noll. Nonsmooth  $\mathcal{H}_\infty$  synthesis. *IEEE Transactions on Automatic Control*, 51(1):71–86, January 2006.
- J. F. Camino, M. C. de Oliveira, and R. E. Skelton. “Convexifying” linear matrix inequality methods for integrating structure and control design. *Journal of Structural Engineering*, 129(7):978–988, 2003.
- K. Galdos, A. Karimi, and R. Longchamp.  $H_\infty$  Controller design for spectral MIMO models by convex optimization. *Journal of Process Control*, 20(10):1175 – 1182, 2010.
- M. Hast, K. J. Åström, B. Bernhardsson, and S. P. Boyd. PID Design By Convex-Concave Procedure. In *2013 European Control Conference*, 2013.
- C.W.J. Hol. *Structured controller synthesis for mechanical servo-systems*. PhD thesis, Delft University of Technology, 2006.
- A. Karimi and G. Galdos. Fixed-order  $H_\infty$  controller design for nonparametric models by convex optimization. *Automatica*, 46(8):1388 – 1394, 2010.
- A. G. J. MacFarlane and I. Postlethwaite. The generalized Nyquist stability criterion and multivariable root loci. *International Journal of Control*, 25(1):81–127, 1977.
- I. Maruta, T.H. Kim, and T. Sugie. Fixed-structure controller synthesis: A meta-heuristic approach using simple constrained particle swarm optimization. *Automatica*, 45(2):553 – 559, 2009. ISSN 0005-1098.
- A. Nemirovskii. Several NP-hard problems arising in robust stability analysis. *Mathematics of Control, Signals and Systems*, 6(2):99–105, 1993. ISSN 0932-4194.
- A. Popov and H. Werner. Efficient design of low-order  $H_\infty$  optimal controllers using evolutionary algorithms and a bisection approach. In *Computer Aided Control System Design, 2006 IEEE International Conference on Control Applications, 2006 IEEE International Symposium on Intelligent Control, 2006 IEEE*, pages 760–765, 2006.
- R.M. Redheffer. On a certain linear fractional transformation. *Journal of Mathematics and Physics*, 39:269–286, 1960.
- M.G. Safonov, K.C. Goh, and J.H. Ly. Control system synthesis via bilinear matrix inequalities. In *American Control Conference, 1994*, pages 45–49, 1994.
- S. Skogestad and I. Postlethwaite. *Multivariable feedback control: analysis and design*. John Wiley & Sons, Chichester, 2006. ISBN 9780471942771.
- E. van Solingen and J.W. van Wingerden. Fixed-structure  $H_\infty$  control design for individual pitch control of two-bladed wind turbines. In *American Control Conference*, 2014.
- K. Zhou and J.C. Doyle. *Essentials of Robust Control*. Prentice Hall International, 1998. ISBN 9780135258330.
- K. Zhou, J.C. Doyle, and K. Glover. *Robust and optimal control*. Prentice Hall, 1996. ISBN 9780134565675.